

FIRST-PRINCIPLES STUDY OF HIGH EXPLOSIVE DECOMPOSITION ENERGETICS

Christine J. Wu and Laurence E. Fried
Lawrence Livermore National Laboratory
P. O. Box 808, Livermore, CA 94550

We have carried out a systematic study of the bond dissociation energies of 15 high explosive molecules using first principles gradient corrected density functional theory. Among them, the mechanism of the gas phase unimolecular decomposition of hexahydro-1,3,5,-trinitro-1,3,5,-triazine (RDX) has been investigated in a detailed fashion. Our results show that the dominant reaction channel is the N-NO₂ bond rupture, which has a barrier of 37.4 kcal/mol and is 18.3 kcal/mol lower than that of the concerted ring fission to three methylenenitramine molecules. We have also identified the weakest bond and calculated the bond strengths for 14 other high explosives. We find that the ratio of the weakest bond strength to the high explosive energy of decomposition may be related to explosive sensitivity.

INTRODUCTION

The molecular decomposition of high explosives has been regarded as an important step in explosive detonation kinetics. In particular, the dissociation energy of the weakest bond of the explosive molecule is expected to play an important role in initiation events. However, previous attempts to correlate bond strengths to impact sensitivity were not successful.¹ Politzer and co-workers have calculated C-NO₂ and N-NO₂ bond dissociation energies of several small and middle size high explosives, from which they concluded that the correlation between bond strength and impact sensitivity is not general, but limited within certain classes of molecules.¹

Given the complexity of detonation chemistry of high explosives, it is not surprising to see that bond dissociation energy alone is not enough to capture high explosive sensitivity, which is likely to be influenced by other energy sources and reaction paths. One such source that we examine in the present study is the energy content of high explosives. We show in this paper that the bond dissociation energy scaled by energy content

is a promising indicator for predicting high explosive sensitivity.

In this paper we investigate the bond dissociation energies of 15 large size high explosive molecules (e.g. > 20 atoms/molecule), many of which have never been calculated using first-principle methods. The first system reported here is a summary report of our previous work of RDX unimolecular decomposition mechanism.² We also extend our RDX results to take into account pressure. Acronyms used in naming the explosives are defined in Table 1. Although RDX is one of the most thoroughly studied energetic compounds, even simple questions, such as the nature of the initial step in the thermal decomposition of RDX, are still a subject of debate.

There are many suggested initial steps in the unimolecular thermal decomposition of RDX. Among them, the most supported mechanisms are (I) N-NO₂ bond rupture, and (II) concerted ring fission to three CH₂N₂O₂ molecules. For instance, a recent supporting evidence for path I was given by the transient IR laser pyrolysis experiments of Wight and Botcher.³ Using a solid

RDX thin film, they found that the initial decomposition products relate mostly to the N-NO₂ bond rupture.³ In addition, their experiments on samples with isotopically labeled nitrogen also showed that decomposition of RDX is mostly unimolecular and involves the removal of only one NO₂.⁴ On the other hand, there is also experimental evidence for path II.⁵ Using infrared multiphoton dissociation (IRMPD) of RDX in a molecular beam, Zhao, Hints and Lee found that a branching ratio of 2:1 for the path II over the path I best matched their time of flight spectra.⁵ Therefore, they concluded that the dominant channel is the symmetric ring-fission II, not the N-NO₂ bond cleavage I.⁵

TABLE 1. ACRONYMS AND ABBREVIATIONS USED FOR HIGH EXPLOSIVE MATERIALS.

DATB	Diaminotrinitrobenzene
DINGU	Dinitroglycourile
EDNA	Ethylenedinitramine
HMX	Octahydro-1,3,5,7-tetranitro-1,3,5,7-tetraazacine
HNB	Hexanitrobenzene
NG	Nitroglycerine
NTO	3-nitro-1,2,4-triazol-5-one
PETN	Pentaerythritol tetranitrate
RDX	Hexahydro-1,3,5-trinitro-1,3,5-triazine
TATB	Triaminotrinitrobenzene
TETRYL	N-methyl-N,2,4,6-tetranitro Benzeneamine
TNA	Trinitroaniline
TNAZ	Trinitroazetidine
TNB	2,4,6-trinitrobenzene
TNT	2,4,6-trinitrotoluene

In this first part of the paper (section A), we present a detailed study of RDX unimolecular dissociation via two competing reaction paths using first-principles gradient-corrected density functional theory (DFT) methods.

DFT methods provide an accurate solution to the Schrodinger equation by postulating an approximate functional relating charge density to energy. Modern functionals depend on the value of the charge density and its gradient. These “gradient corrected” functionals are found to yield enhanced accuracy in the prediction of many molecular properties over “local” functionals that depend only on the value of the charge density. A range of basis sets and modern gradient corrected density functional methods were applied to RDX, in order to ensure that the final conclusion does not depend on computational methods.

Once we determined the minimum basis set and the functional for reliably predicting bond dissociation

energy, we apply them to calculate bond dissociation energies of other 14 common high explosive molecules ranging from highly sensitive (e.g. HNB) to insensitive ones (e.g. TATB). The first six high explosive molecules are nitrated aromatic benzene rings: TATB, DATB, TNA, TNB, TNT, and HNB. We also have molecules that are saturated cyclic nitramines: HMX and RDX. In addition, we included TNAZ, NTO, EDNA, DINGU, PETN, NG and TETRYL. We use the homolysis bond dissociation energies to identify the weakest bond. Our goal is to find out whether there is a relation between the strength of the weakest chemical bond of a high explosive molecule, its energy content, and its impact sensitivity.

CALCULATIONAL DETAILS

All total energy calculations were performed using the Gaussian 94/DFT package with spin-polarized gradient-corrected exchange and correlation functionals.⁶ In the calculations of RDX decomposition, we have chosen four widely adopted and promising functionals: B-PW91, B3-PW91, B-LYP and B3-LYP. B refers to the Becke’s 1988 gradient-corrected exchange functional⁷ which reproduces the exact asymptotic behavior of exchange-energy density in finite system, and B3 is denoted for the Becke’s hybrid method⁸ of mixing Hartree-Fock exchange energy into the exchange functional. PW91 and LYP are the gradient-corrected correlation functionals of Perdew-Wang,⁹ and Lee, Yang and Parr.¹⁰ Three Gaussian-type basis sets were used for the Kohn-Sham orbital expansion: Dunning’s valence double zeta (D95V),¹¹ D95V plus diffuse function (D95V+),¹¹ and Dunning’s most recent correlation consistent polarized valence double zeta basis sets (cc-pVDZ).¹²

In the comparative study of bond dissociation energies of a series of high explosives, we have used the D95V basis set and the B-PW91 functional, as we found them to give qualitatively correct results for the bond dissociation energies of RDX. Zero point energy corrections were not included, since we do not expect these small energy corrections to affect the qualitative results.

RESULTS AND DISCUSSION

A. RDX Decomposition Mechanism

The results for the N-NO₂ bond dissociation energy (D) are presented in Table 2. D_e and D₀ refer to the values without and with zero point correction of the vibrational energy, respectively, which was calculated at the B-PW91/D95V level. It is satisfying to see that the four functionals we used give consistent results. Although adding polarization functions has a larger effect than adding diffuse functions, neither changes the value of D significantly. For instance, the largest deviation between D95V and D95V+ is −0.9 kcal/mol (B-LYP),

while that between D95V and cc-pVDZ is -2.6 kcal/mol (B-LYP). The deviation between the basis sets considered is roughly the same as the deviation between the functionals. Becke's hybrid B3 method gives a slightly higher value of the bond energy (about 3 kcal/mol) than Becke 88. Using our largest basis set (cc-pVDZ), four functionals give D_e ranging from 39.5 to 43.3 kcal/mol, with an average value of 41.8 kcal/mol and the maximum deviation of ± 2.3 kcal/mol. Taking the zero point energy correction into account, we predict that the N-NO₂ bond energy D_0 is 37.4 kcal/mol at the B-PW91/cc-pVDZ level.

TABLE 2. CALCULATED RDX N-NO₂ BOND DISSOCIATION ENERGY (D) AND HEAT OF REACTION (E) FOR RDX RING FISSION DISSOCIATION PATHWAY.

Calculation	D_e (D_0)	ΔE_c (ΔE_0)
B-PW91/D95V	41.6 (37.1)	63.7 (54.5)
B-PW91/D95V+	41.2 (36.7)	59.5 (50.3)
B-PW91/cc-pVDZ	41.9 (37.4)	54.2 (45.0)
B-LYP/ D95V	42.1 (37.6)	51.3 (42.1)
B-LYP/ D95V+	41.2 (36.7)	48.9 (39.7)
B-LYP/ cc-pVDZ	39.5 (35.0)	45.5 (36.3)
B3-PW91/D95V	43.6 (39.1)	77.8 (68.6)
B3-PW91/D95V+	44.3 (39.8)	74.9 (65.7)
B3-PW91/cc-pVDZ	43.3 (38.8)	66.0 (56.8)
B3-LYP/ D95V	42.4 (37.9)	69.1 (59.9)
B3-LYP/ D95V+	41.9 (37.4)	64.3 (55.1)
B3-LYP/ cc-pVDZ	42.5 (38.0)	58.3 (49.1)

Our DFT values of the N-NO₂ bond energy in RDX are significantly smaller than the previous estimate of 48 kcal/mol,¹³ which was based on the assumption that the N-NO₂ bond in RDX is similar to that of methyl-nitramine and nitramine. We have performed the same level of calculations on methyl-nitramine and nitramine and found that RDX has a weaker N-NO₂ bond than nitramine and methyl-nitramine due to both geometric and electronic relaxations through the RDX ring fragment (H₆C₃N₅O₄). Our estimate for the RDX geometric stabilization is between 2–6 kcal/mol. Electronic relaxation is thus the dominant mechanism; it accounts for 6–10 kcal/mol.

The adiabatic potential energy curve of breaking of N-NO₂ bond (shown in Figure 1) was obtained by optimizing the geometry at each fixed N-NO₂ separation at the B-PW91/D95V level. We found the potential energy profile has zero barrier (the typical case for a radical recombination reaction). This is in agreement with the experimental observation that the product translational energy distribution for N-NO₂ bond rupture is peaked at

zero. Therefore, the barrier for breaking the N-NO₂ bond is approximately equal to N-NO₂ bond energy D_0 .

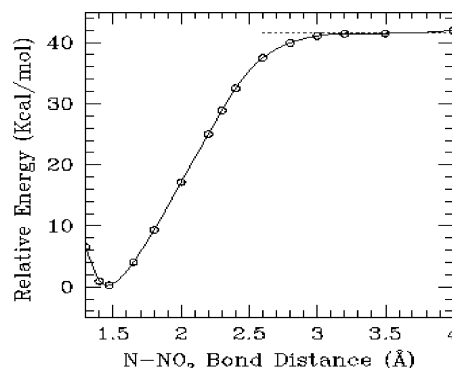


FIGURE 1. POTENTIAL ENERGY CURVE OF RDX DISSOCIATION VIA N-NO₂ BOND RUPTURE ALONG THE REACTION COORDINATE (N-NO₂ BOND).

The heat of reaction (ΔE) for the concerted symmetric ring fission II is also listed in Table 2. ΔE_c and ΔE_0 refer to the values without and with zero point correction of the vibrational energy, respectively. It was calculated in the same fashion as the N-NO₂ bond dissociation energy. Note that the deviation between various exchange-correlation functionals and basis sets are larger than for pathway I. This perhaps is due to the large change in the electronic character from RDX to H₂CNNO₂. However, this pathway involves rearrangement of three chemical bonds. If one estimates the deviations between functionals and basis sets based on the unit of changing bond, they are not too far from those of pathway I. For instance, Becke's hybrid method (B3) again gives consistently higher values (about 4 kcal/mol per bond) than Becke 88. Nevertheless, the heat of reaction for the ring fission is systematically higher than the N-NO₂ bond dissociation energy within the same functional and basis set. Using the largest basis set cc-pVDZ, four functionals give ΔE_c ranging from 66.0 to 45.5 kcal/mol, with an average value of 56.0 and maximum deviation of ± 10.5 kcal/mol. Taking the zero point energy correction of 9.2 kcal/mol, our best estimate for the heat of reaction of the concerted ring fission is at the B-PW91/cc-pVDZ level is 45.0 kcal/mol.

We then mapped the potential energy profile of the ring fission (see Figure 2) in order to identify the transition state. The reaction coordinate parameter β is chosen to be the three alternate C-N distances along the breaking C-N bonds (indicated as the dashed line in Figure 2). At each β , we optimized all other degrees of freedom at both B-PW91/D95V and B-PW91/D95V+ level. Although

adding diffuse functions lowers the potential energy, the energy profiles of the D95V and D95V+ basis sets have a similar shape, including the same β of 2.21 Å at the saddle point. We have assumed that cc-pVDZ has the same β value for the saddle point, therefore the transition state at cc-pVDZ level is obtained by optimizing all other degree of freedoms while keeping β at 2.21 Å. This B-PW91/cc-pVDZ calculation gives a transition state height of 61.3 kcal/mol. The Hessian calculation at the B-PW91/D95V level shows one imaginary frequency for the predicted transition state. Taking into account the zero point energy correction, our best estimate of barrier height at B-PW91/cc-pVDZ level for pathway II is 55.7 kcal/mol. Note that this value is about 17 kcal/mol smaller than the previous LDA result.¹⁴

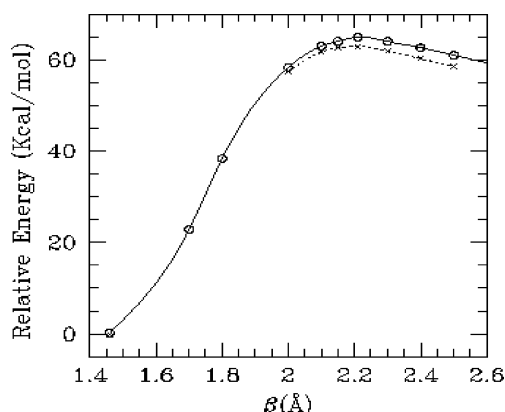


FIGURE 2. POTENTIAL ENERGY CURVE FOR RDX RING FISSION REACTION ALONG THE REACTION COORDINATE (THE BROKEN C-N BOND, β).

A detailed comparison between path I and path II requires the evaluation of not only the barriers, but also the reaction prefactors. We used a simple kinetic theory to estimate the reaction prefactor for path I. The Gorin¹⁵ model was applied, in which the reaction is assumed to proceed when the attractive force between fragments is larger than the centrifugal force. For path II, harmonic transition state theory was applied. Further details of the prefactor calculations are given in Ref. 2. We estimated the prefactors to be 7×10^{17} and $1 \times 10^{17} \text{ s}^{-1}$ for channel I and II, respectively. Since the prefactors for path I and II are of the same order of magnitude, we predict path I to be the dominant channel due to its lower activation barrier.

The effect of pressure on activation barrier is estimated by $H^{\text{act}} = E^{\text{act}} + PV^{\text{act}}$, where H^{act} , E^{act} , V^{act} are activation enthalpy, energy and volume, respectively. We computed volumes using Monte-Carlo integration of electron charge density at the BPW91/D95V level. Note

in Figure 1 that one cannot locate the exact transition state of a simple N-NO₂ bond scission based on the adiabatic potential energy curve, since the barrier for the backward reaction is negligible. We have assume that the true transition state is somewhere close to the beginning of the plateau, for instance $R(\text{N} - \text{NO}_2) = 3.2 \text{ Å}$. We estimated the activation volume of the path I from the volume of $R(\text{N} - \text{NO}_2) = 3.2 \text{ Å}$. Figure 3 plots activation enthalpy as a function of pressure. We found that the activation volumes for path I and II are 5.6 and 6.2 cm³/mol, respectively. Therefore, path I has a lower barrier than path II even under pressure.

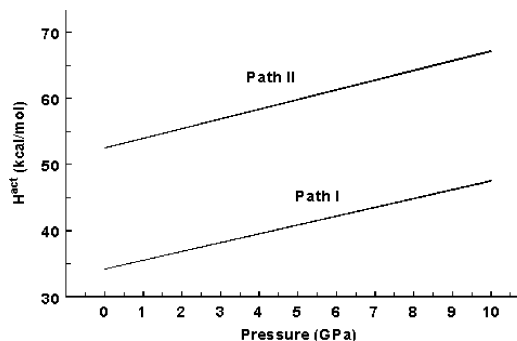


FIGURE 3. ACTIVATION ENTHALPY AS A FUNCTION OF PRESSURE FOR PATH I AND II.

B. Bond Dissociation Energies of other 14 High Explosives

DFT bond dissociation energies of the nitrated aromatic benzene rings: TATB, DATB, TNA, TNB, TNT and HNB are displayed in Table 3 to 8. We found that C-NO₂ is the weakest bond for all molecules in this group. As we expected, having NH₂ adjacent to NO₂ increases the stability of the C-NO₂ bond due to hydrogen bonding between NH₂ and NO₂. For instance, the strength of the weakest C-NO₂ bond of TNB, TNA, DATB and TATB increases from 67.7, 71.6, 74.6 to 77.2 kcal/mol as the number of NH₂ groups increases from 0 to 3. We find that each NO₂-NH₂ hydrogen bond increases the bond dissociation energy by 2–4 kcal/mol. The hydrogen bond lengths for this group of molecules are also in the typical range. For TATB, the distance between O of NO₂ and H of the adjacent NH₂ is 1.691 Å.

The second weakest bond for TATB, TNA and DATB is the C-NH₂ bond, which varies slightly from 124.1, 128.8 to 131.1 kcal/mol, respectively. Note that the C-NH₂ groups of TATB, TNA and DATB have identical nearest neighbors indicating the localized nature of the C-NH₂ bonding. C-NH₂ bond strengths are significantly

(about 50 kcal/mol) stronger than those of C-NO₂ due to the electronic relaxation of the NO₂ fragment. The difference between C-NO₂ and C-NH₂ bond strengths is also reflected in the C-N separations (R). For instance, R(C-NH₂) of TATB is 0.095 Å shorter than R(C-NO₂) of 1.446 Å. Within this group, the values of R(C-NO₂) and R(C-NH₂) do not vary significantly.

TABLE 3. DFT BOND DISSOCIATION ENERGIES (D, KCAL/MOL) AND BOND LENGTHS (R, Å) IN TATB.

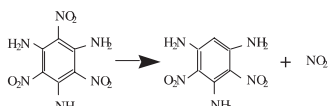
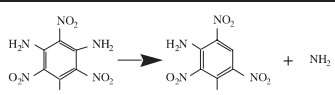
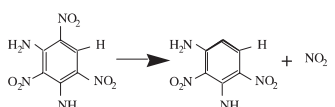
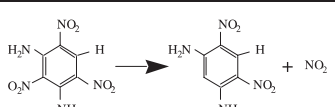
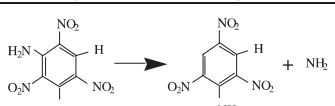
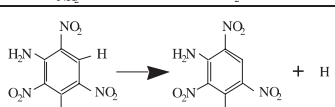
Decomposition Pathways	BPW91/D95V
	D(C-NO ₂) = 77.2 R(C-NO ₂) = 1.446
	D(C-NH ₂) = 124.1 R(C-NH ₂) = 1.351

TABLE 4. DFT BOND DISSOCIATION ENERGIES (D, KCAL/MOL) AND BOND LENGTHS (R, Å) IN DATB.

Decomposition Pathways	BPW91/D95V
	D(C-NO ₂) = 74.6 R(C-NO ₂) = 1.469
	D(C-NO ₂) = 76.1 R(C-NO ₂) = 1.451
	D(C-NH ₂) = 128.8 R(C-NH ₂) = 1.351
	D(C-H) = 152.0 R(C-H) = 1.092

C-H (C is a ring Carbon) bonds are the strongest for this group of high explosive molecules. Note that C-H bond strengths of TNA, MATB, TNB and TNT are similar (154.3, 152.9, 152.0, 151.9 kcal/mol, respectively) as they have a similar local bonding environment. In comparison, the C-H bond from the CH₃ group of TNT is about 30 kcal/mol weaker than those of C(ring)-Hs. This difference reflects the fact that sp² C forms a stronger bond with H than sp³ C.

For TATB, DATB, TNA, TNB and TNT, we found that the NO₂ and NH₂ functional groups on the six-carbon ring lay in almost the same plane as the ring. The planar arrangement promotes hydrogen bonding between NO₂ and NH₂ and the electron conjugation effect between NO₂ and the benzene ring. We can estimate the magnitude of the electron conjugation effect as follows. The barrier for NO₂ rotation to a perpendicular geometry in TNB is 18 kcal/mol. From this, we estimate that the magnitude of the electron conjugation effect is roughly 6 kcal/mol.

TABLE 5. DFT BOND DISSOCIATION ENERGY (D, KCAL/MOL) AND BOND LENGTHS (R, Å) IN TNA.

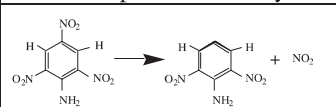
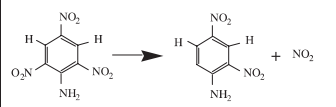
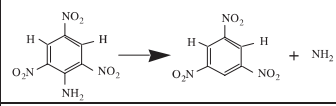
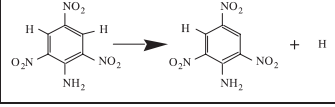
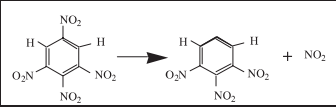
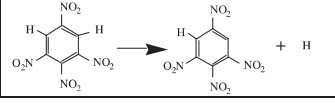
Decomposition Pathways	BPW91/D95V
	D(C-NO ₂) = 71.6 R(C-NO ₂) = 1.481
	D(C-NO ₂) = 71.1 R(C-NO ₂) = 1.478
	D(C-NH ₂) = 131.0 R(C-NH ₂) = 1.353
	D(C-H) = 152.9 R(C-H) = 1.092

TABLE 6. DFT BOND DISSOCIATION ENERGIES (D, KCAL/MOL) AND BOND LENGTHS (R, Å) IN TNB.

Decomposition Pathways	BPW91/D95V
	D(C-NO ₂) = 67.7 R(C-NO ₂) = 1.498
	D(C-H) = 154.3 R(C-H) = 1.091

For HNB, which has six NO₂ groups, intramolecular repulsions between the NO₂ groups prevent a planar equilibrium geometry. We found that the lowest energy structure has alternating in plane and out of plane NO₂ groups. This structure is 0.6 kcal/mol lower in energy than the planar structure. Thus the planar structure, although not a minimum, should be thermally accessible

in HNB. The low barrier to rotation is indicative of a lack of NO₂ conjugation.

In Table 7, we list bond dissociation energies of C-NO₂ for the three NO₂ groups that are perpendicular to the plane. In comparison, the C-NO₂ bonds where the NO₂ groups are in plane are 4.7 kcal/mol stronger, which is consistent with the electron conjugation effect of 6 kcal/mol per NO₂ estimated from TNB.

The results for HMX and TNAZ are listed in Table 9 and 10, respectively. The N-NO₂ bond strength of HMX was calculated to be 42.8 kcal/mol at the BPW91/D95V level, which is similar to that of RDX (45.0 kcal/mol at the same level of calculation). For TNAZ, we have found that the N-NO₂ is stronger than the C-NO₂ bond by about 3 kcal/mol, in contrast to an observation that the C-NO₂ bond is typically stronger than the N-NO₂ bond.

TABLE 7. DFT BOND DISSOCIATION ENERGIES (D, KCAL/MOL) AND BOND LENGTHS (R, Å) IN TNT.

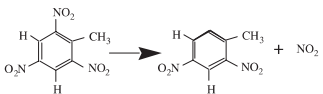
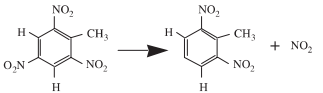
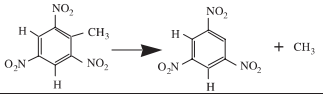
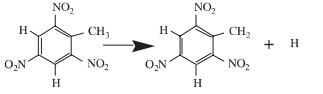
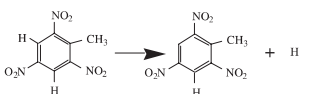
Decomposition Pathways	BPW91/D95V
	D(C-NO ₂) = 62.4 R(C-NO ₂) = 1.512
	D(C-NO ₂) = 67.0 R(C-NO ₂) = 1.492
	D(C-CH ₃) = 102.3 R(C-CH ₃) = 1.514
	D(C-H) = 123.8 R(C-H) = 1.107
	D(C-H) = 151.3 R(C-H) = 1.091

TABLE 8. DFT BOND DISSOCIATION ENERGIES (D, KCAL/MOL) AND BOND LENGTHS (R, Å) IN HNB.

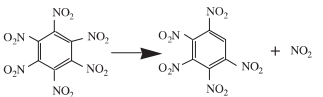
Decomposition Pathways	BPW91/D95V
	D(C-NO ₂) = 43.8 R(C-NO ₂) = 1.518

TABLE 9. DFT BOND DISSOCIATION ENERGIES (D, KCAL/MOL) AND BOND LENGTHS (R, Å) IN HMX.

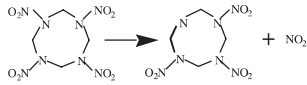
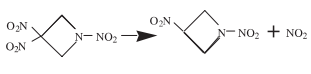
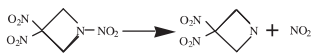
Decomposition Reaction	BPW91/D95V
	D(N-NO ₂) = 42.8 R(N-NO ₂) = 1.422

TABLE 10. DFT BOND DISSOCIATION ENERGIES (D, KCAL/MOL) AND BOND LENGTHS (R, Å) IN TNAZ.

Decomposition Reaction	BPW91/D95V
	D(C-NO ₂) = 39.8 R(C-NO ₂) = 1.560
	D(N-NO ₂) = 43.9 R(N-NO ₂) = 1.424

We have listed the calculated (BPW91/D95V level) strengths of the weakest bond (N-NO₂ or C-NO₂) and impact sensitivities in Table 11. Note that the compounds NTO, EDNA, DINGU, PETN and NG are also included in Table 11. The impact sensitivity measurements are taken from the LLNL Explosives Handbook¹⁶, the Navy Explosives Handbook¹⁷, and Kohler and Meyer¹⁸. Note that these types of measurements are typically rough. Measured impact sensitivities depend strongly on the apparatus used and the experimental protocol. We used LLNL measurements using a number 12 tool and a 2.5 kg weight wherever possible to minimize these differences. Also, values from Kohler and Meyer were scaled to a reference of HMX in order to convert from their effective impact energies (in N-m) to drop hammer heights in cm. No scaling of the Navy values was necessary, since Navy values for HMX match those of LLNL closely.

There appears to be some relation between De and explosive sensitivity, but it is clearly not the only controlling factor. For instance, HNB is the most sensitive material in the comparison study, but has a De value similar to the much less sensitive DINGU. Nitrobenzene compounds, which are the least sensitive compounds studied here, are found to have the highest De values.

It is clear that the energy content of the material must also play a role in determining the impact sensitivity. It is well known that high energy materials tend to be the most sensitive. We have determined the energy content of the explosives studied here with the Cheetah 2.0 thermochemical code¹⁹. The Cheetah code was used to determine E_d, the energy of decomposition into equilibrium

products at standard state. This is a measure of the total energy content of the material. We display the results of these calculations in Table 11. Energy content can be used to explain some of the apparent anomalies in the D_e results. For instance, although HNB has a typical D_e value, it has the greatest energy content.

TABLE 11. BOND STRENGTH (D_e , KCAL/MOL) OF THE WEAKEST BOND, ENERGY CONTENT (E_d , KJ/CC) AND IMPACT SENSITIVITY (I, CM) OF HIGH EXPLOSIVES.

HE	Weakest Bond	D_e	E_d	I *
TATB	C-NO ₂	77.2	8.6	>320
DATB	C-NO ₂	74.6	8.6	>320
TNA	C-NO ₂	71.6	8.1	177(N)
NTO	C-NO ₂	67.8	7.7	>280
TNB	C-NO ₂	67.7	8.6	100(N)
TNT	C-NO ₂	62.4	7.7	148
EDNA	N-NO ₂	49.4	9.2	35 (K)
HNB	C-NO ₂	43.8	14.3	8.5
DINGU	N-NO ₂	43.1	8.5	24 (K)
HMX	N-NO ₂	42.8	11.1	32
RDX	N-NO ₂	41.6	10.4	28
TNAZ	C-NO ₂	39.8	11.2	29
PETN	O-NO ₂	39.8	10.5	14
NG	N-NO ₂	37.6	10.0	20
TETRYL	N-NO ₂	28.7	8.8	37

* (K) indicates values from Kohler and Meyer. (N) indicates values from the Navy Explosives Handbook. All other data was taken from LLNL measurements.

In Figure 4 we show scatter plots to help visualize the results of Table 11. Note that a logarithmic axis is used to represent the drop hammer values (H_{50}). D_e is seen to be useful in separating the very insensitive materials such as TATB, DATB, TNA, and NTO. Within the group of more sensitive materials, however, there seems to be little apparent relation between D_e and H_{50} .

The opposite conclusion appears to be true of the energy of decomposition E_d . The relationship between E_d and impact sensitivity appears to be strongest for materials that are very high in energy, while becoming more constant at larger H_{50} values.

The ratio between D_e and E_d could be an important quantity in determining the impact sensitivity. The physical motivation for this is that D_e plays the role of an activation barrier. Once a microscopic region ignites in

response to mechanical deformation, the energy released by the reaction is controlled by E_d . This will in turn control the local temperature and the likelihood of a propagating chemical reaction. Arrhenius kinetics depend on the ratio of activation barrier to temperature, thus motivating our study of the D_e/E_d ratio here. We caution the reader, however, that the use of D_e as an overall reaction barrier for explosive decomposition is certainly an oversimplification. Nonetheless, we find that D_e/E_d is a more nearly linear function of $\log(H_{50})$ than D_e or E_d individually.

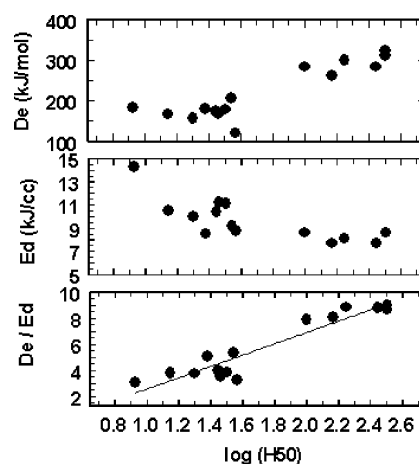


FIGURE 4. BOND DISSOCIATION ENERGIES (D_e), DECOMPOSITION ENERGIES (E_d) AND THE RATIO D_e/E_d ARE PLOTTED VERSUS THE LOG OF THE DROP HAMMER HEIGHT.

CONCLUSION

In the present paper, we have undertaken a study of bond dissociation in a wide variety of energetic materials. We began with a detailed study of decomposition in RDX. We found that the activation barrier for concerted ring fission is roughly 18 kcal/mol greater than that for N-NO₂ bond rupture. This suggests that thermal gas phase decomposition most likely proceeds via N-NO₂ bond rupture.

We have also performed a comparative study of bond dissociation energies in a wide range of energetic materials. We found that there is some apparent relation between the strength of the weakest bond and sensitivity, but that other factors play a role. In particular, we showed that the ratio of the bond dissociation energy to the explosive decomposition energy seems to be a reasonable practical indicator of explosive sensitivity. Since this indicator is easily computed with electronic structure and

thermochemical codes, it may prove useful in the design of new energetic materials. We note, however, that explosive sensitivity also depends on particle morphology and other factors that are not taken into account in the present work. Incorporating these factors is a challenge for future study in this area.

ACKNOWLEDGMENTS

This work was performed under the auspices of the U. S. Department of Energy by the Lawrence Livermore National Laboratory under contract No. W-7405-ENG-48. We thank P. Clark Souers and Rosalind Swansiger for providing us impact sensitivity measurements.

REFERENCES

1. Politzer P. and Murray J. S., *J. Mol. Struct.*, **376**, 419 (1996).
2. Wu C. J. and Fried L. E., *J. Phys. Chem.*, **101**, 8675 (1997). "A correction to RDX total energy at the BPW91/cc-pVDZ level (from -897.47526 to -897.480308) has been sent to *J. Chem. Phys.* for Ref. 2. Values reported in Ref. 2 that are relative to this total energy should increase by 3.2 kcal/mol."
3. Wight C. A. and Botcher T. R., *J. Am. Chem. Soc.*, **114**, 8303 (1992).
4. Botcher T. R. and Weight, C. A., *J. Phys. Chem.*, **98**, 5541 (1994).
5. Zhao X. S., Hints E. J. and Lee Y. T., *J. Chem. Phys.*, **88**, 801 (1988).
6. Frisch M. J., Trucks G. W., Schlegel H. B., Gill, P. M. W., Johnson B. G., Robb M. A., Cheeseman J. R., Keith T. A., Petersson G. A., Montgomery J. A., Raghavachari K., Al-Laham M. A., Zakrzewski V. G., Ortiz J. V., Foresman J. B., Cioslowski, J., Stefanov B. B., Nanayakkara A., Challacombe M., Peng C. Y., Ayala P. Y., Chen W., Wong M. W., Andres J. L., Replogle E. S., Gomperts R., Martin R. L., Fox D. J., Binkley J. S., Defrees D. J., Baker J., Stewart J. P., Head-Gordon M., Gonzalez C. and Pople J. A., *Gaussian 94*, Gaussian, Inc., Pittsburgh, PA, 1995.
7. Becke A. D., *Phys. Rev. A*, **38**, 3098 (1988).
8. Becke A. D., *J. Chem. Phys.*, **98**, 5648 (1993).
9. Lee C., Yang W., and Parr R. G., *Phys. Rev. B*, **37**, 785 (1988).
10. Perdew J. P. and Wang Y., *Phys. Rev. B*, **45**, 13244 (1992).
11. Dunning Jr. T. H. and Hay P. J., *Modern Theoretical Chemistry*, Plenum: New York, 1976.
12. Dunning Jr. T. H., *J. Chem. Phys.*, **90**, 1007 (1989).
13. Melius, C. F. and Binkley, J. S., Twenty-first Symposium (International) on Combustion, The Combustion Institute, 1986, p. 1953.
14. Habibollahzadeh D., Grodzicki M., Seminario J. M., and Politzer P., *J. Phys. Chem.*, **95**, 7699 (1991).
15. Gorin E., *Acta Physicochem. U.R.S.S.*, **9**, 661 (1938).
16. Dobratz, B.M. and Crawford, P. C. "LLNL Explosives Handbook", LLNL Report UCRL-52997, 1985.
17. Hall, T.N. and Holden, J.R. "Navy Explosives Handbook: Explosion Effects and Properties Part III", Naval Surface Warfare Center Report NSWC MP88-116, 1985.
18. Kohler J. and Meyer R., *Explosives*, VCH Publishers: Weinheim, 1993.
19. Fried, L. E., Howard, W. M. and Souers, P. C., "CHEETAH 2.0 User's Manual", Lawrence Livermore National Laboratory Report UCRL—MA-117541 Rev. 5, 1998.